JOC The Journal of Organic Chemistry

Article

pubs.acs.org/joc

Selectivities of Multicomponent [4 + 2]/[3 + 2] Cycloadditions of 3-Nitroindole with Substituted Alkenes: A DFT Analysis

Hélène Gérard*,† and Isabelle Chataigner*,‡

†Laboratoire de Chimie Théorique UMR 7616, UPMC Univ Paris 06, F-75005 Paris, France

‡Laboratoire COBRA, CNRS UMR 6014 & FR 3038, Université de Rouen, 76821 Mont St Aignan, France

Supporting Information

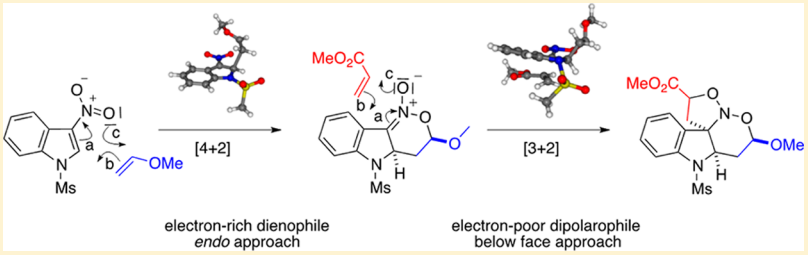

ABSTRACT: The chemo-, regio-, and stereoselectivities of multicomponent [4 + 2]/[3 + 2] domino cycloaddition reactions involving nitroindole derivatives with vinylethers and acrylates are studied computationnally and compared to experimental results. In this process, the nitroarene first reacts as an electron-deficient heterodiene with the electron-rich alkene following an inverse electron-demand [4 + 2] process, leading to a nitronate intermediate in a fully selective way. This intermediate exclusively interacts, in a second step, with the electron-deficient alkene and undergoes a chemo- and regioselective [3 + 2] cycloaddition. The density functional theory calculations reported in this Article fully account for the selectivities observed experimentally. Electronic displacements along the reaction path are examined using a topological analysis of the electron-localization function (ELF). The first [4 + 2] reaction follows a classical concerted, although asynchronous process, which is reliably described by the frontier molecular-orbital (FMO) model. In contrast, the electronic displacements observed during the second [3 + 2] step are unexpected, involving an electron donation by the electron-deficient reaction partner.

INTRODUCTION

Multicomponent reactions (MCR) have emerged as efficient methods for the generation of elaborated compounds from simple organic building blocks.[1] In particular, MCR involving domino pericyclic reactions are valuable tools because they take advantage of the high selectivities generally observed for these processes. We recently reported that nitroindole **E1**[2] efficiently reacts with substituted alkenes **E2** and **E3** in a [4 + 2]/[3 + 2] cycloaddition cascade[3] to afford adduct **E4** in a chemo- regio- and stereoselective manner (Scheme 1).[4] In the sequence, the primary [4 + 2] cycloaddition exclusively involves enol ether **E2** and appears to be completely endo selective. The susbequent [3 + 2] process involves acrylate **E3** and shows a total facial selectivity, setting the stereochemistry at the ring junction, with an endo/exo selectivity that depends on the acrylate substituent. The nitrosoketals **E4** thus generated can undergo a second domino process involving an N−O bonds cleavage/cyclization/reduction/lactamisation sequence to yield a tetracyclic dearomatized diamine featuring a quaternary center at the ring junction (Scheme 1). In two simple operations, a tetracyclic-dearomatized diamine featuring a tetrasubstituted center at the ring junction is thus efficiently generated.

Scheme 1

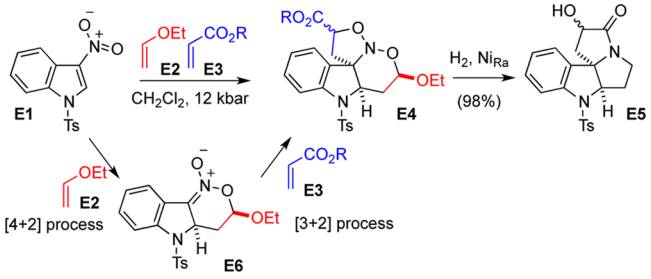

The complete chemo- and regioselectivities of both [4 + 2] and [3 + 2] cycloaddition reactions of this MCR process are quite interesting from a synthetic point of view, leading to the formation of a single compound among the 2^4 possibilities. A better understanding of the mechanistic details of this domino process would thus provide helpful pieces of information for the further development of these cascade cycloaddition routes.

DFT calculations on hetero Diels−Alder (HDA) reactions involving nitroolefins and electron-rich alkenes have been reported in the literature.[5] Monosubstituted alkenes were reported to lead to a preferred ortho regioselectivity (with the alkene substituent in the α position of the cyclic oxygen atom),

Received: July 9, 2013
Published: August 5, 2013

Scheme 2

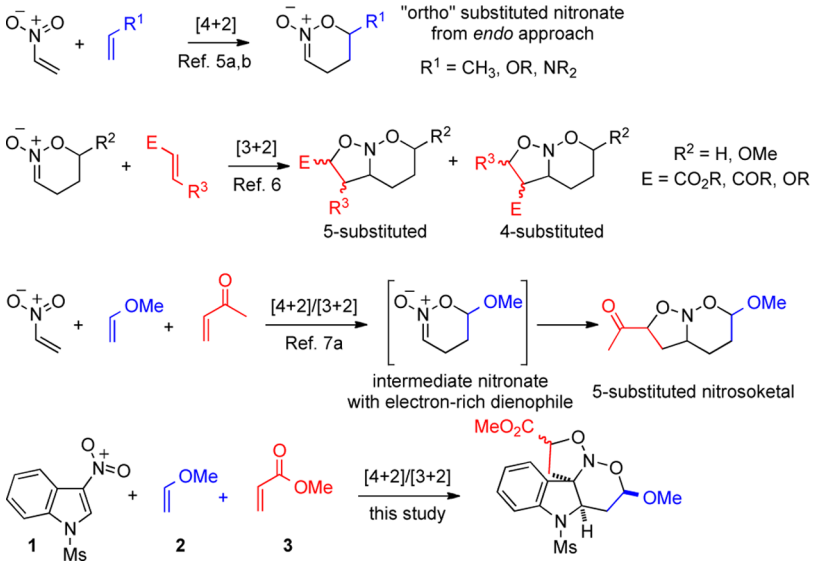

especially when the dienophile bears highly electron-releasing groups. An endo approach was computationally preferred, in line with the experimental observations (Scheme 2), and a concerted, although asynchronous pathway has been proposed for these reactions. Some [3 + 2] cycloadditions involving neutral nitronate dipoles have also been examined by computational means.[6] The regioselectivity of this process varied with the substitution of the dipolarophile involved in the reaction. In fact, monosubstituted alkenes were shown to give five-substituted isoxazoline, whereas 1,2-disubstituted alkenes gave regioisomeric mixtures of cycloadducts, depending upon the electronic and steric nature of both E and R^3 (Scheme 2). The combination of these two cycloaddition processes in tandem [4 + 2]/[3 + 2] reactions have been described computationally in a few cases.[7,8] Domingo and co-workers studied the chemo-, regio-, and stereoselectivities of the intermolecular process involving nitroethene, methylvinylether, and methylvinylketone. Here again, the first HDA reaction using nitroethene as an electron-deficient heterodiene was favored in the presence of the electron-rich alkene, generating the ortho-substituted nitronate bearing an axial methoxy group arising from a preferred endo approach. In contrast, the subsequent [3 + 2] cycloaddition process involved the electron-poor monosubstituted alkene partner and led to the five-substituted cyclic nitrosoketal. A preferred exo approach was computed in this case (Scheme 2).

To get insight into the mechanistic details of the domino [4 + 2]/[3 + 2] cascade involving nitroheteroarenes, whose electronic and steric features were quite different from the model nitroethene used in previous studies, we have undertaken a DFT study of these cycloadditions. Our main objective was to explain the course of this multicomponent reaction that led to the exclusive formation of nitrosoketals **E4** from a nitroarene compound and two different alkenic components, **E2** and **E3**. These studies were carried out on a model, although realistic, system involving 3-nitroindole **1** (bearing a methanesulfonyl protecting group on the nitrogen atom instead of a *p*-methylbenzenesulfonyl), methyl vinyl ether **2** (instead of ethyl vinyl ether), and methyl acrylate **3**. In this domino process, we first considered the [4 + 2] cycloaddition and studied the chemo-, regio-, and stereoselectivities of this reaction by comparing the reactivities of the electron-rich and electron-poor dienophilic partners computationally. Next, the selectivities of the subsequent [3 + 2] cycloaddition were studied. Here again, the possible involvement of both alkenes as dipolarophiles was considered. In each case, detailed descriptions of the electronic rearrangements during the course of the reactions were examined to propose realistic working models.

RESULTS AND DISCUSSION

First-Step: [4 + 2] Cycloaddition. With a qualitative description of cycloadditions most commonly undertaken via a frontier molecular orbital (FMO) model, the FMO energies of the three components involved in this step were first evaluated (Table 1). This preliminary work pointed to a preferential

Table 1. Frontier MO Energies of Substrates 1, 2, 3, and 8

entry	substrate	E_{HOMO} (eV)	E_{LUMO} (eV)
1	**1**	−6.71	−2.35
2	**2**	−6.13	−1.18
3	**3**	−7.40	−1.24
4	**8**[a]	−5.69	−0.42

[a]For the formula of **8**, see Scheme 4.

interaction between the lowest unoccupied MO (LUMO) of the heterodienic partner **1** and the highest occupied MO (HOMO) of the dienophilic partner (**2** or **3**, $\Delta\Delta E$ = 1.27 eV in favor of **2**). Thus, this HDA reaction followed the expected inverse electron-demand process. The smaller energy difference between LUMO(**1**) and HOMO(**2**) (3.78 eV) with respect to LUMO(**1**) and HOMO(**3**) (5.05 eV) likely indicated a preferential involvement of electron-rich dienophile **2** in this first step.

The regiochemistry of the process should be governed by the coefficients of the involved MO for each substrate (Figure 1). The shapes of LUMO(**1**) and HOMO(**2**) exhibited a larger extension on the C2 atoms for each substrate[9] so that the formation of cycloadducts featuring a new σ bond between these two carbon atoms was predicted. Experimentally, the isolation of nitrosoketals **E4** was in line with this expected regiochemistry.

A quantitative evaluation of the selectivity of this [4 + 2] process was then attempted. Taking into consideration that the reaction was under kinetic control, we undertook the localization

dx.doi.org/10.1021/jo401482b | J. Org. Chem. 2013, 78, 9233−9242

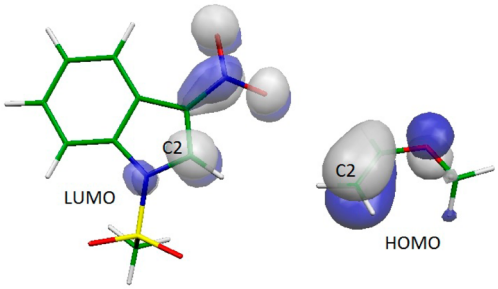

Figure 1. Extensions of LUMO(**1**) and HOMO(**2**).

of the transition states (TS) of the heterocycloaddition between indole **1** and dienophiles **2** or **3**. In each case, combining the two regioisomeric approaches with the two diastereoisomeric endo/exo approaches led to eight different TS (Scheme 3, Table 2). Channels 1 and 2 were found to be highly favored over the other possible pathways, leading to the preferred formation of nitronates *endo*-**4** and *exo*-**4**. A remarkably high-energy difference was observed between the two regiochemical courses of the process ($\Delta\Delta G^{\ddagger} = 16.40$ kcal mol^{-1}) (Table 2, compare channel 1 with 3 and channel 2 with 4), which is fully in line with the exclusive formation of nitronate **E6**. A slightly smaller but still significant energy preference was obtained for the chemoselectivity of the process, as the TS for dienophile **2** in the regio-1 orientation were more stable (by 9.98 kcal mol^{-1}) than those of dienophile **3** (Table 2, compare channel 1 with 5 and channel 2 with 6). These figures were also in line with the experimental results that allowed the isolation of the nitrosoketal arising from a primary cycloaddition with **2** only.[4] Considering this first step, the difference between the activation energies of the endo and exo attacks was found to amount to 1.30 kcal mol^{-1} in favor of the endo approach. This endo preference could arise from the positive interaction between the oxygen atom of the vinyl ether dienophile and the nitrogen atom of the nitro group of the diene arising in this approach (Figure 2).[5,7] This slight difference was also in good agreement with the experimental results: the high-pressure reaction led to the exclusive formation of the endo stereoisomer, whereas a 90:10 mixture of stereoisomers was isolated when the cycloaddition was performed under reflux of toluene.[4,10]

Even if the reaction was computed to proceed through a concerted mechanism, the TS were found to be asynchronous (Figure 2). This asynchronicity was proposed to be associated with a strong charge transfer at the TS so that this reaction can be considered as a polar Diels–Alder according to a classification on the basis of these criteria.[11] The consequences of this feature in terms of the electronic rearrangements along the reaction path were examined using a topological analysis of the electron localization function (ELF), which allowed quantification of the weight of the various mesomeric forms in a Lewis-like description of the electronic density.[12] Recently, this method has been widely used to describe the electronic reorganizations for model Diels–Alder[13] and hetero-Diels–Alder reactions.[14] To avoid the analysis of the mechanism in a sum of "microsteps", we chose to summarize all of the single events described in previous reports in major rearrangements that could help to render the mechanism easily tractable. Their modulations also aimed at understanding the selectivity issues (chemo-, regio-, and stereoselectivities). The populations of the valence basins, to be regarded as the number of electrons associated with the bonds and lone pairs, are plotted in Figure 3 (a detailed description is given in the Supporting Information). The computations highlighted three major events: (a) At reaction coordinate (RC) −0.3 Å, the C2–C3 bond of the indolic ring (**1**: B (C2, C3)) went from double (a population of more than three electrons) to single (about two electrons), in association with an increase of the C3–N2 bond basins (**1**: B (C3, N2));[15] this step was thus summarized by arrow a in Figure 3, where electrons of the C2═C3 bond were transferred to C3–N2. (b) Around RC 0.0 Å (and thus quasisimultaneous to step a), the creation of the first bonding basin between the two fragments was observed, with formation of the C2–C2 bond (**1**–**2**: B (C2, C2)) through the fusion of two pseudoradical centers observed on these two atoms only at the transition state. Simultaneously, the population

Scheme 3. Possible Reaction Pathways for the First Step of the Domino [4 + 2]/[3 + 2] Process

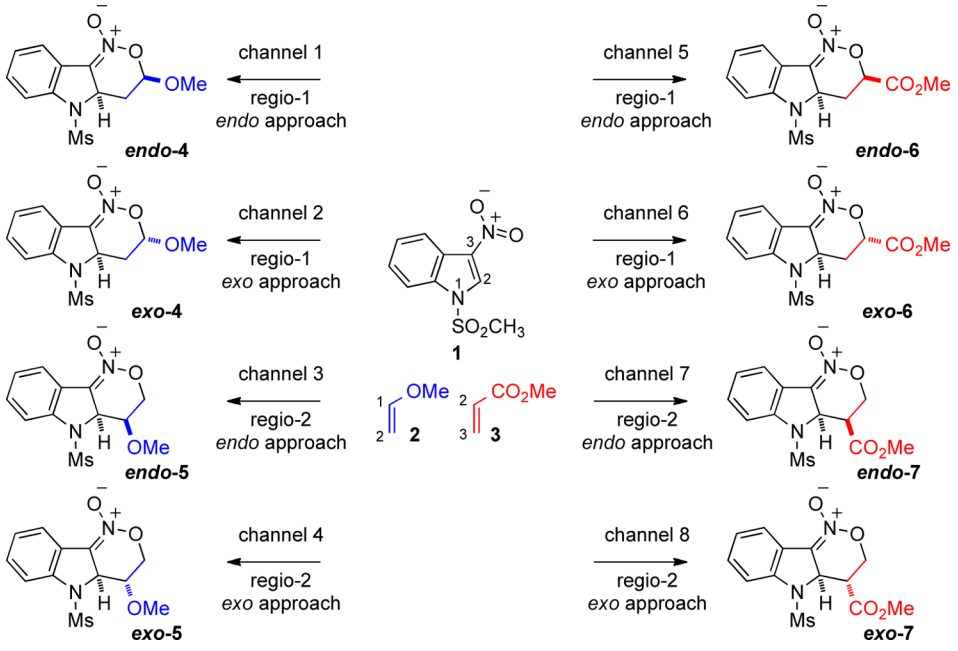

dx.doi.org/10.1021/jo401482b | J. Org. Chem. 2013, 78, 9233–9242

Table 2. First Step: [4 + 2] Cycloaddition Involving Substrates 1 and 2 or 3

channel	dienophile	regiochemistry	approach	$\Delta G^{\ddagger}$ (kcal mol^{-1})	$\Delta\Delta G^{\ddagger}$ (kcal mol^{-1})[a]	ΔG_r (kcal mol^{-1})
1	**2**	regio-1	endo	23.72	0	−2.94
2	**2**	regio-1	exo	25.02	1.30	−0.94
3	**2**	regio-2	endo	40.12	16.40	7.16
4	**2**	regio-2	exo	41.37	17.65	8.45
5	**3**	regio-1	endo	33.70	9.98	5.84
6	**3**	regio-1	exo	33.95	10.23	6.57
7	**3**	regio-2	endo	33.83	10.11	6.59
8	**3**	regio-2	exo	34.23	10.51	6.12

[a]Energy difference with the most favorable process (channel 1).

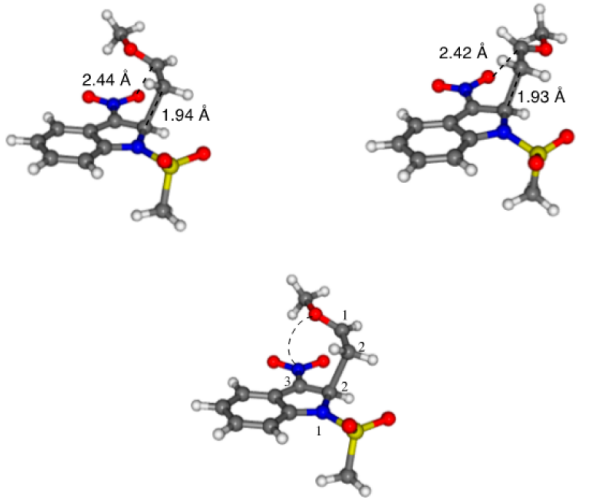

Figure 2. TS for channels 1 and 2 (top; defined in scheme 3). Positive interaction between the nitrogen and oxygen atoms of **1** and **2**, respectively (bottom).

of the C1−C2 bond of the vinylether moiety (**2**: B (C1, C2)) was significantly depleted, leading to a partial breaking of this bond. This reaction step can thus be described by arrow b, which summarizes a nucleophilic attack of vinylether on an electrophilic indole, in line with an inverse-demand reaction path. After the initial events, this transformation went on smoothly until the last step. (c) The electronic rearrangement ended around RC 0.7 Å with the formation of the second intermolecular bond (**1**−**2**: B (O1,C1)) associated with a decrease of the population of the valence basins of the oxygen atom lone pair. This step can thus be represented by arrow c.

Overall, Figure 3 illustrates the three major events of this step: the polarization of the heterodiene followed by the formation of the C−C bond and finally that of the C−O bond. This order of events was in line with the displacements expected from the FMOs. A highly similar scheme was obtained for the exo process (Supporting Information, Figure FS2). This contrasted, however, with the formation of the other possible compound, **5**, involving electron-deficient alkene **3** as the dienophile (channel 5, Scheme 3 and Table 2). In this case, the C−C bond that formed through the merging of two carbon

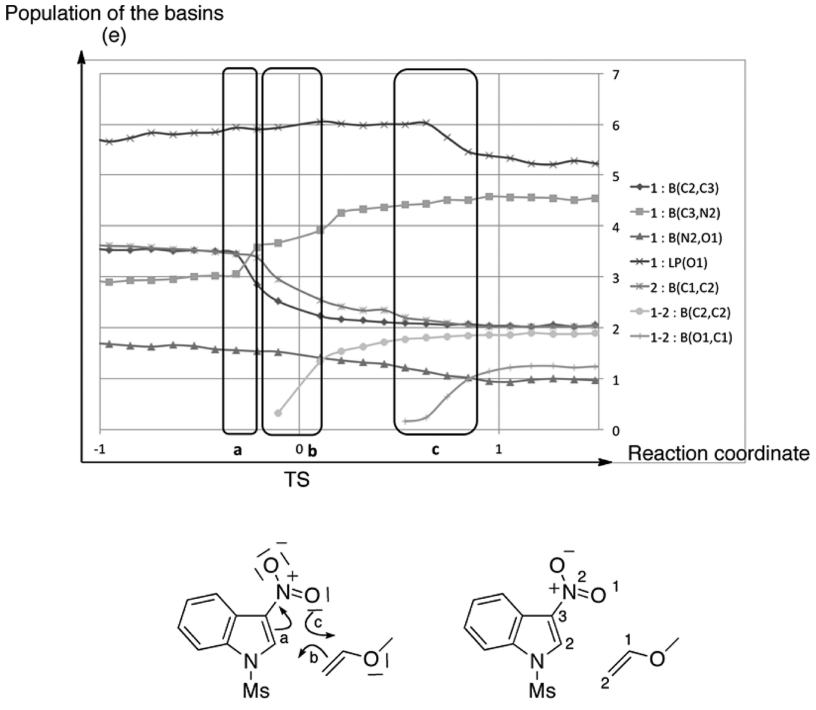

Figure 3. Population (in electrons) of the various basins involved in reaction 1 → 4 following the numbering presented in the bottom of the figure as a function of the reaction coordinate (in Å, increasing from reactant to product, 0 is for the transition state). A schematic description of the reaction is shown at the bottom.

dx.doi.org/10.1021/jo401482b | J. Org. Chem. 2013, 78, 9233−9242

Scheme 4. Possible Regiochemical Pathways for the [3 + 2] Process Involving Model Nitronate 8 and Dipolarophiles 2 or 3

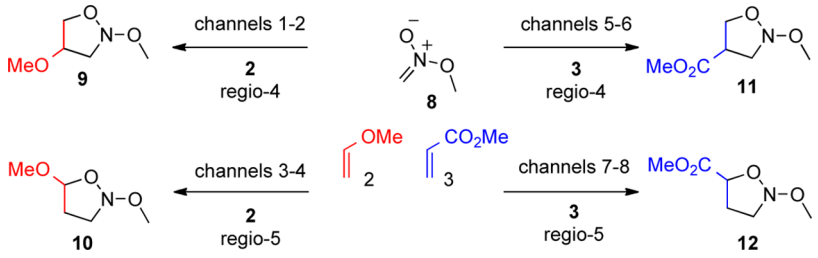

pseudoradical centers (step b) was simultaneous to the C−O bond formation (step c) (See the Supporting Information for the values, Figure FS3). This feature could explain the absence of regioselectivity observed for the reaction of **3** with **1** (Table 2, compare channels 5 and 6 with 7 and 8), which is in strong contrast with the cycloaddition of **2** to **1**, where steps a and b were quasisynchronous and c took place later. The preferred process could be thus described as highly asynchronous, fully regioselective, and governed by a nucleophile/electrophile attack.

[3 + 2] Model Cycloaddition. For the sake of CPU saving, small model nitronate **8** was first considered to get initial insight on the [3 + 2] cycloaddition process (Scheme 4). The chemoselectivity of this reaction step was evaluated by comparing the possible implication of **2** or **3** as electron-rich or electron-poor dipolarophilic partners through the determination of the FMO energies of the substrates (Table 1). The energy difference between HOMO(**8**) and LUMO(**3**) with respect to HOMO(**8**) and LUMO(**2**) (5.05 and 5.11 eV, respectively) expectedly indicated a preferential involvement of electron-poor dipolarophile **3** in this second [3 + 2] cycloaddition process. However, the difference between the LUMO energy levels of the alkenes remained small. In addition, the difference between LUMO(**8**) and HOMO(**2**) (5.71 eV) was in the same range. This pointed to the higher competition between **2** or **3** in this second-step process. These results were in line with the experimental observations showing that when the reaction was performed in the absence of any electron-poor alkene, vinylether was involved both as a dienophile and dipolarophile in the first [4 + 2] and in the second [3 + 2] steps, respectively.[16] As a consequence, a full quantitative evaluation of the chemoselectivity was carried out for the considered transformation (vide infra). Considering the regioselectivity of this [3 + 2] cycloaddition reaction, previous studies have shown the preference for the formation of the five-substituted regioisomers.[6,17] Computations of the extensions of LUMO(**3**) and HOMO(**8**) showed a larger coefficient of C3 and C1 respectively, which is in line with this expected regiochemistry and the experimental isolation of nitrosoketals **E4** exclusively (Figure 4).

The complete reaction sequence between model nitronate **8** and dipolarophiles **2** and **3** was next studied. The two regioisomeric approaches (leading to the formation of four-substituted or five-substituted isoxazoles) combined with the two endo/exo approaches led to eight different TS (Scheme 4 and Table 3).[18,8] The chemoselectivity of the [3 + 2] process was shown to favor the involvement of electron-poor dipolarophile **3** (Table 3, compare channels 1−4 with 5−8). The energy difference was, however, relatively small ($\Delta\Delta G^{\ddagger}$ = 1.99 kcal mol^{-1}), and this chemoselectivity issue needed to be re-examined when considering the more complex nitronate *endo*-**4** (vide infra). The [3 + 2] cycloaddition favored the formation of the

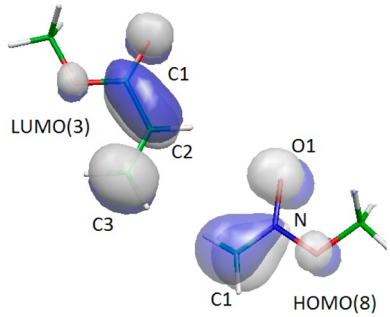

Figure 4. Extensions of LUMO(**3**) and HOMO(**8**).

five-substituted regioisomers regardless of the dipolarophile involved (Table 3, compare channels 1 with 3, 2 with 4, 5 with 7, and 6 with 8). The energy difference in this case was the largest ($\Delta\Delta G^{\ddagger}$ = 2.54 kcal mol^{-1}), which is in line with the experimental results that led to the exclusive formation of the five-substituted regioisomers. The difference between the activation energies of the endo and exo attacks amounted to 1.46 kcal mol^{-1} in favor of the exo approach (Table 3, channels 7 and 8).

Second Step: [3 + 2] Cycloaddition. An evaluation of the preferred [3 + 2] process was then undertaken with the indole derived nitronate *endo*-**4**. Considering the results observed with model nitronate **8**, the chemoselectivity of the process was studied with dipolarophiles **2** and **3** to generate the five-substituted regioisomers. In each case, the two face approaches combined with two diastereoisomeric endo/exo approaches allowed for eight different TS (Scheme 5 and Table 4).[18,8]

The approach of the dipolarophile from the face below, opposite to the methoxy substituent on the intermediate nitronate, appeared to be highly favored, by more than 8 kcal mol^{-1} (compare channels 1 and 2 with 3 and 4 and channels 5 and 6 with 7 and 8 in Table 4). This large energy difference explained the exclusive formation of the steroisomer bearing a cis stereochemistry at the ring junction of the generated nitrosoketal and suggested that no alternative face of attack was possible here. As expected from the MO energy levels, the activation energy difference between the processes involving dipolarophiles **2** and **3** was not as marked (2.44 kcal mol^{-1}) (Table 4, compare channels 3 and 8); however, it was in favor of the formation of "mixed" nitrosoketals **16**, as experimentally observed. The smaller energy difference ($\Delta\Delta G^{\ddagger}$ = 1.23 kcal mol^{-1}) for the endo versus exo approaches were in line with the experimental results that allowed the isolation of the nitrosoketals as endo/exo mixtures (from 55:45 to 78:22 with indole substrates, depending on the ester substituent on the acrylate partner, and an exo preference of 25:75 with pyrrole substrates).[4] The reaction was found to proceed through a concerted mechanism, and the TS were slightly asynchronous (Figure 5). These structural features

dx.doi.org/10.1021/jo401482b | J. Org. Chem. 2013, 78, 9233−9242

Table 3. Regiochemistry of the [3 + 2] Cycloaddition Involving Model Substrates 8 and 2 or 3

channel	dienophile	approach	$\Delta G^{\ddagger}$ (kcal mol^{-1})	$\Delta\Delta G^{\ddagger}$ (kcal mol^{-1})[a]	ΔG_r (kcal mol^{-1})
1	**2**	regio-4, endo	29.09	9.70	−12.74
2	**2**	regio-4, exo	27.74	8.35	−11.99
3	**2**	regio-5, endo	23.02	3.63	−20.72
4	**2**	regio-5, exo	21.38	1.99	−21.03
5	**3**	regio-4, endo	21.93	2.54	−15.07
6	**3**	regio-4, exo	22.78	3.39	−14.84
7	**3**	regio-5, endo	20.85	1.46	−15.30
8	**3**	regio-5, exo	19.39	0	−14.96

[a]Energy difference with the most favorable process (channel 8).

Scheme 5. Possible Reaction Pathways for the Second Step of the Domino [4 + 2]/[3 + 2] Process

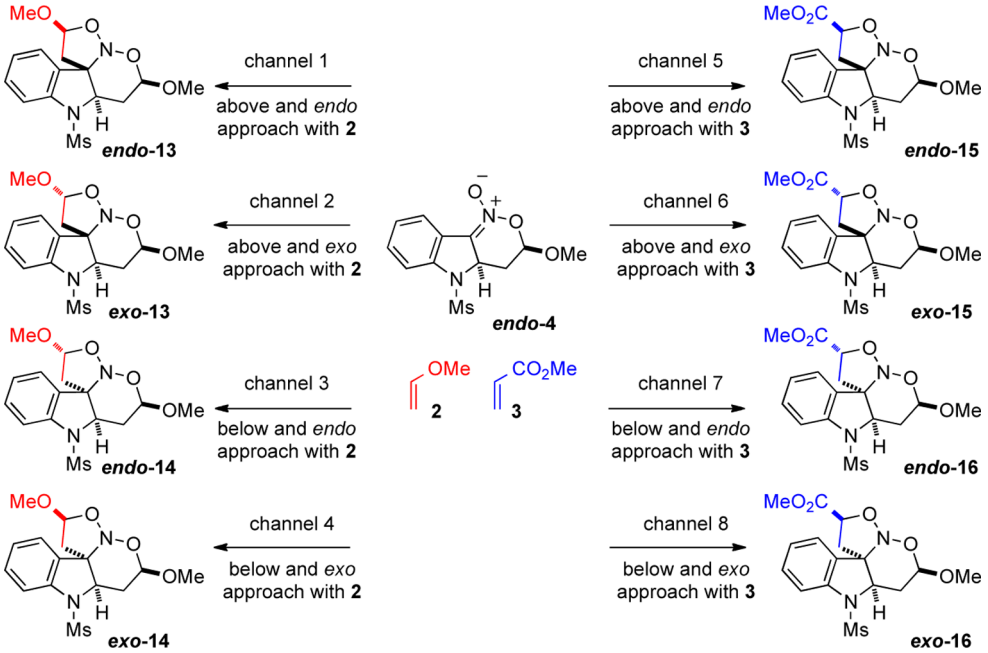

Table 4. Second Step: [3 + 2] Cycloaddition Involving Substrates *endo*-4 and 2 or 3

channel	dienophile	approach	$\Delta G^{\ddagger}$ (kcal mol^{-1})	$\Delta\Delta G^{\ddagger}$ (kcal mol^{-1})[a]	ΔG_r (kcal mol^{-1})
1	**2**	above, endo	36.14	13.05	2.43
2	**2**	above, exo	33.80	10.71	0.30
3	**2**	below, endo	25.53	2.44	−10.59
4	**2**	below, exo	28.17	5.08	−6.35
5	**3**	above, endo	35.84	12.75	8.94
6	**3**	above, exo	33.53	10.44	6.29
7	**3**	below, endo	**24.32**	1.23	−5.25
8	**3**	below, exo	**23.09**	0	−4.08

[a]Energy difference with the most favorable process (channel 8).

were proposed to be associated with a small charge transfer at the TS and with nonpolar mechanisms.[19]

The electronic rearrangements occurring during [3 + 2] cycloadditions were previously studied in depth.[20] A detailed scheme for the electronic reorganization during the reaction course[20a] and a study of the role played by the pseudoradical character of the starting materials in the decrease of the reaction barrier were proposed.[20b] Here again, we decided to focus on the major events of this second step. As described in Figure 6, three events were obtained, in close agreement with the mechanism observed previously, for the first step: (a) A decrease of the C3═N2 bond population (**4**: B (C3,N2)) from 4.5 to 3 electrons, and

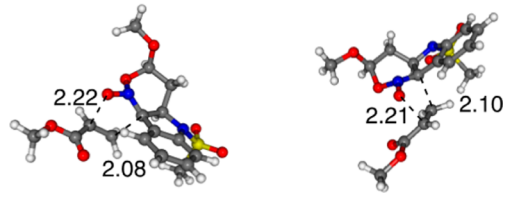

Figure 5. C2−O2 and C3−C3 bond distances (Å) in the TS for channels 7 and 8 (defined in Scheme 5).

the formation of a lone pair on N2 (**4**: LP (N2)) for a RC of about −0.9 Å were observed, which is in line with the polarization

dx.doi.org/10.1021/jo401482b | J. Org. Chem. 2013, 78, 9233−9242

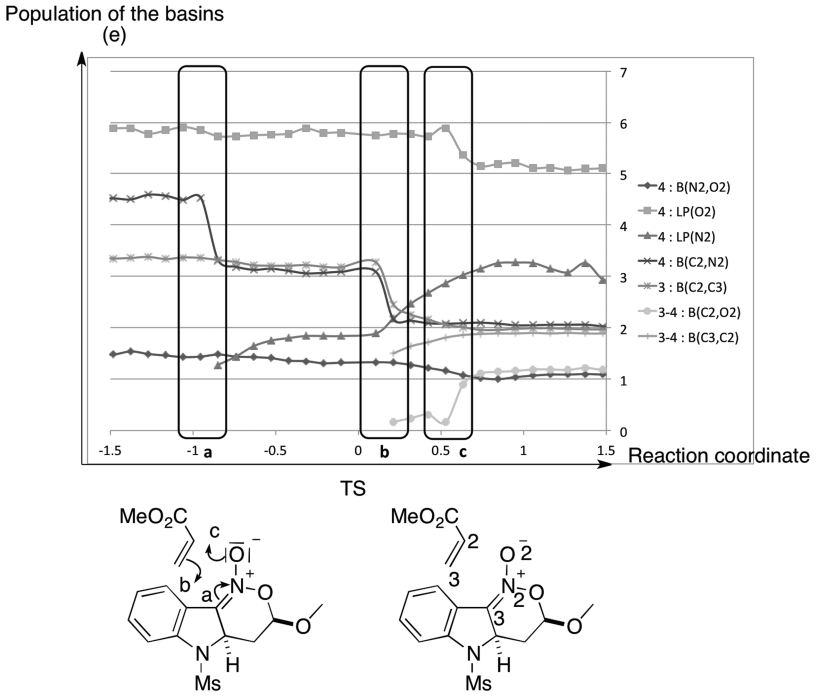

Figure 6. Population (in electrons) of the various basins involved in the reaction **4** → **16**, following the numbering presented in the Figure (below), as a function of the reaction coordinate (in Å, increasing from reactant to product, 0 is for the transition state). Below, schematic description of the reaction.

of the double bond proposed in step a. (b) The formation of the first interfragment bond between the two carbon atoms (**3**−**4**: B (C3,C3)) for a RC of about 0.2 Å, which is associated with the cleavage of the olefinic C2═C3 double bond (**3**: B (C2,C3)) and an enrichment of the nitrogen lone pair (LP (N2)), as summarized by arrow b. A detailed description showed that this bond was obtained from the fusion of two pseudoradical centers at each carbon atom (Figure FS4, Supporting Information). (c) Finally, for a RC of 0.6 Å, the formation of the C2−O2 bond (**3**−**4**: B(C2, O2)) by transfer of part of the population of the O lone pairs (**4**: LP(O2)), according to the electronic movement of step c.

In this situation, the dipolarophile thus played the role of the electron donor, in contrast with the electron demand expected from the MO energies, but consistently with the potential competition between the two processes, as explained above. The fact that steps b and c were not initiated at the TS was fully in line with the absence of charge transfer at that point, as proposed from the geometry and the literature.[19,20b] We note that a similar description was obtained in the case of model nitronate **8** (Table 3, channel 8, and Figure FS5, Supporting Information) and for the reaction involving vinylether **2** (Table 4, channel 3, and Figure FS6, Supporting Information), except that for the reaction coordinate values and for the details of step b, as in these two cases, no enrichment of the LP (N2) was observed. These results can also be compared to the description of the 1,3-dipolar cycloaddition between fulminic acid and acetylene published by Polo et al. for which similar LP (N), B (C−C), and B (C−O) formations were also observed, but for which the B (C−N) and B (C−C) bond breaking were found to be monotonous during the reaction course, with no abrupt B (C−C) formation step. The preferred process for the second step could thus be described as quasisynchronous and slightly exo-selective, with an unexpected electron donation from electron-deficient partner **3**. The overall reaction profile is presented in Figure 7.

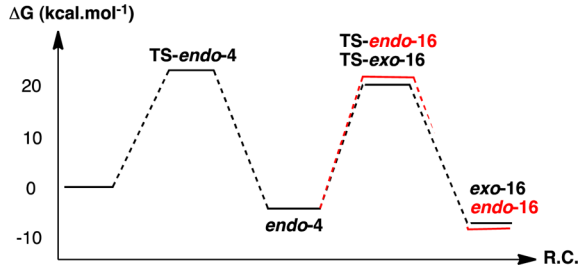

Figure 7. Energy profile of the overall [4 + 2]/[3 + 2] process.

CONCLUSIONS

The results described in this Article analyze the selectivities observed in the [4 + 2]/[3 + 2] cycloaddition involving nitroindoles, electron-rich and electron-poor alkenes. They show the mechanisms through which this multicomponent process can lead to a single reaction product. The primary [4 + 2] reaction involves the nitroarene as an electron-poor heterodiene that preferentially interacts with an electron-rich dienophile following an inverse electron-demand HDA process. Chemo- and regioselectivities are total, and the large energy differences between the possible TS suggest that no alternative pathways are to be considered for this step. The endo approach is favored, which explains the formation of the nitronate compound bearing an axial alkoxy group. Considering the stereochemistry of this reaction, the smaller energy preference for the endo approach suggests that structural alterations of the electron-rich dienophile could trigger different endo/exo stereochemistries. The electronic rearrangements observed during the reaction course are in line with the expected pathway and, for this first cycloaddition process, the FMO model provides perfectly reliable predictions. In contrast, during the second [3 + 2] cycloaddition step, unexpected electronic rearrangements are observed. Even if electron-deficient acrylate **3** appears to react in preference to electron-rich vinyl ether **2** with the intermediate

dx.doi.org/10.1021/jo401482b | J. Org. Chem. 2013, 78, 9233−9242

Table 5. Validation of the Computational Level by Comparing the Energy Differences between the Endo and Exo Channels for the First and Second Steps

entry	method	$\Delta\Delta G^{\ddagger}_{\text{first step}}$ (kcal mol^{-1})[a]	$\Delta\Delta G_{\text{r first step}}$ (kcal mol^{-1})[a]	$\Delta\Delta G^{\ddagger}_{\text{second step}}$ (kcal mol^{-1})[a]	$\Delta\Delta G_{\text{r second step}}$ (kcal mol^{-1})[a]
1	B3LYP/6-31G**	1.30	2.00	1.23	1.17
2	B3LYP/6-31+G**	0.40	2.03	0.97	1.83
3	B3LYP/6-31G**[c]	0.66	2.07	0.47	0.90
4	B3PW91/6-31G**	1.98	1.61	1.63	1.86
5	B97D/6-31G**	1.18	2.10	0.86	1.39

[a]Energy difference between channels 1 and 2 of Table 2. [a]Energy difference between channels 7 and 8 of Table 4. [c]Calculations affected by applying the conductor polarizable continuum model (CH_2Cl_2).

nitronates (*endo*-**4** or **8**), the calculations demonstrate that the electron-poor dipolarophile provides the electrons to the electron-rich dipole. This counterintuitive behavior thus shows that classical models on the basis of static polarizations (electrostatic or orbital control) or on the usually admitted electron flows are not reliable to predict selectivities in this case and that an understanding of the nature of the electronic rearrangements remains associated with the quantitative localization of the TS. More reliable descriptions can be obtained from an additional description of intermolecular interactions.[21] The evolution of the latter along the reaction path is currently under study and will be published in due time.

COMPUTATIONAL METHODS

Computations were run using the Gaussian 09 set of programs, revision B.01.[22] Geometry optimizations were carried out in absence of symmetry constraints. The nature of the TS was checked via harmonic-frequency evaluations to show the presence of one and only one imaginary frequency. These harmonic frequencies were used unscaled for the evaluation of the thermodynamic data of the reaction. They were computed using the standard Gaussian procedure (T = 298, 15 K, and P = 1 atm). The B3LYP/6-31G(d,p) level of theory[23] was used for the study because it is compatible with the numerous arrangements we had to take into account and has been shown to be a reliable method for similar organic[24] and dipolar systems.[25] Additional validation of this computational level was carried out on the endo/exo selectivity (TS and reaction energy) of the first and second reaction steps, which exhibited the smaller energy differences. The results are gathered in Table 5 and showed that, despite an energy difference smaller than 0.9 kcal·mol^{-1}, the trend was maintained when modifying the basis set and the DFT and when taking PCM into account.

To confirm connectivity between reactant and products, the TS structures were given small geometrical perturbations along the reaction coordinates and then further geometrical optimizations were carried out to ensure that they connect the reactant and product of interest. Under these conditions, the TS were found to connect to precomplexes in both the first and second step. These structures were weakly bonded, as evidenced from the long distance between the two fragments and the small exothermicity associated (about 4 kcal mol^{-1} but never larger than 8.10 kcal mol^{-1}). As a consequence, the activation/reaction Gibbs free energies were computed as the difference between the separated reactants and the TS/product. As all examined processes were associative in these conditions, corrections to the Gibbs free energy because of the high pressure were only connected to the loss of the translational entropy of one molecule[26] so that the $\Delta\Delta G$ between the experimental pressure (12 000 atm) and the computed one (1 atm) was constant and equal to $Nk_BT\ln(P_{high}/P_{1\ atm})$, which was evaluated to be 5.57 kcal mol^{-1}. All values given in the tables take this correction into account. Moreover, the energy difference between the separated reactants and the precomplexes (and thus the reaction path) was subjected to a basis set superposition error (BSSE). To estimate the magnitude of the BSSE, the counterpoise approximation using the standard Gaussian procedure in the case of the channels 1 and 2 of Table 2 was evaluated.[27] Quasi-identical values were obtained for the two processes (3.7 kcal mol^{-1} for channel 1 and 3.4 kcal mol^{-1} for channel 2), allowing us to consider the energy of the starting material to be overestimated by about 3.5 kcal mol^{-1}. As this value was significantly smaller than all of the barriers computed, it was not included in the values presented above.

Intrinsic reaction coordinate (IRC) calculations were carried out using a step size of 0.2 Bohr and computing the force constants at every step. Because the reaction did not involve the modification of a single internal coordinate (asynchronicity of the formation of the two bonds), the composition of the reaction coordinate (RC) had to be modified and thus re-evaluated as the reaction proceeded. To provide an analysis of the electronic structure, the topological analysis of the ELF (electron localization function)[28] was performed using the TopMod package[29] for all points on the reaction path. Within this framework, space was partitioned into basins of attractors that could be classified as core basins surrounding nuclei and valence basins. It has been shown that the latter could be identified, depending of the number of core basins with which they shared a common boundary (synaptic order), with either atomic lone-pair (LP (X)) for monosynaptic V (X) valence basins or bonding regions between two atoms, X and Y, (B(X,Y)) for disynaptic V (X,Y) basins.[12]

ASSOCIATED CONTENT

Supporting Information

Total energy and Cartesian coordinates for **1**, **2**, **3**, TS-*endo*-**4**, TS-*exo*-**4**, TS-*endo*-**5**, TS-*exo*-**5**, **TS**-*endo*-**6**, TS-*exo*-**6**, TS-*endo*-**7**, TS-*exo*-**7**, *endo*-**4**, *exo*-**4**, *endo*-**5**, *exo*-**5**, *endo*-**6**, *exo*-**6**, *endo*-**7**, *exo*-**7**, **8**, TS-*endo*-**9**, TS-*exo*-**9**, TS-*endo*-**10**, TS-*exo*-**10**, TS-*endo*-**11**, TS-*exo*-**11**, TS-*endo*-**12**, TS-*exo*-**12**, *endo*-**9**, *exo*-**9**, *endo*-**10**, *exo*-**10**, *endo*-**11**, *exo*-**11**, *endo*-**12**, *exo*-**12**, TS-*endo*-**13**, TS-*exo*-**13**, TS-*endo*-**14**, TS-*exo*-**14**, TS-*endo*-**15**, TS-*exo*-**15**, TS-*endo*-**16**, TS-*exo*-**16**, *endo*-**13**, *exo*-**13**, *endo*-**14**, *exo*-**14**, *endo*-**15**, *exo*-**15**, *endo*-**16**, and *exo*-**16**. Complete description of the evolution of the basins population (in electrons) for the first step, channels 1, 2 and 5, for the second step, on the model dipole 8, channel 8 and for the second step on the complete system, channels 3 and 8. This material is available free of charge via the Internet at http://pubs.acs.org.

AUTHOR INFORMATION

Corresponding Author

*E-mail: helene@lct.jussieu.fr (H.G.), isabelle.chataigner@univ-rouen.fr (I.C.).

Notes

The authors declare no competing financial interest.

ACKNOWLEDGMENTS

We are grateful to the CRIHAN (Saint Etienne du Rouvray, France) for the generous allocation of computer time.

REFERENCES

(1) For general reviews, see: (a) *Multicomponent Reactions*; Zhu, J., Bienaymé, H., Eds.; Wiley-VCH: Weinheim, Germany, 2005. (b) *Tetrahedron* **2005**, *61*, 11299−11520. (c) Shiri, M. *Chem. Rev.*

2012, *112*, 3508−3549. (d) de Graaff, C.; Ruijter, E.; Orru, R. V. A. *Chem. Soc. Rev.* **2012**, *41*, 3969−4009. (e) Pellissier, H. *Chem. Rev.* **2013**, *113*, 442−524.

(2) E numbering refers to compounds used experimentally.

(3) For a review, see: (a) Denmark, S. E.; Thorarensen, A. *Chem. Rev.* **1996**, *96*, 137−165. Also, see: (b) Denmark, S. E.; Thorarensen, A.; Middleton, D. S. *J. Am. Chem. Soc.* **1996**, *118*, 8266−8277. (c) Denmark, S. E.; Thorarensen, A. *J. Am. Chem. Soc.* **1997**, *119*, 125−137. (d) Denmark, S. E.; Parker, D. L.; Dixon, J. A. *J. Org. Chem.* **1997**, *62*, 435−436. (e) Denmark, S. E.; Marcin, L. R. *J. Org. Chem.* **1997**, *62*, 1675−1686. (f) Denmark, S. E.; Dixon, J. A. *J. Org. Chem.* **1997**, *62*, 7086−7087. (g) Uittenbogaard, R. M.; Seerden, J.-P. G.; Scheeren, H. W. *Tetrahedron* **1997**, *53*, 11929−11936. (h) Denmark, S. E.; Middleton, D. S. *J. Org. Chem.* **1998**, *63*, 1604−1618. (i) Denmark, S. E.; Hurd, A. R. *J. Org. Chem.* **1998**, *63*, 3045−3050. (j) Denmark, S. E.; Martinborough, E. A. *J. Am. Chem. Soc.* **1999**, *121*, 3046−3056. (k) Kuster, G. J. T.; Kalmoua, F.; de Gelder, R.; Scheeren, H. W. *Chem. Commun.* **1999**, 855−856. (l) Denmark, S. E.; Seierstad, M. *J. Org. Chem.* **1999**, *64*, 1610−1619. (m) Denmark, S. E.; Hurd, A. R. *J. Org. Chem.* **2000**, *65*, 2875−2886. (n) Kuster, G. J.; Scheeren, H. W. *Tetrahedron Lett.* **2000**, *41*, 515−519. (o) Denmark, S. E.; Cottell, J. J. *J. Org. Chem.* **2001**, *66*, 4276−4284. (p) Denmark, S. E.; Gomez, L. *Org. Lett.* **2001**, *3*, 2907−2910. (q) Denmark, S. E.; Guagnano, V.; Vaugeois, J. *Can. J. Chem.* **2001**, *79*, 1606−1616. (r) Kuster, G. J. T.; Steeghs, R. H. J.; Scheeren, H. W. *Eur. J. Org. Chem.* **2001**, 553−560. (s) Denmark, S. E.; Gomez, L. *Heterocycles* **2002**, *58*, 129−136. (t) Denmark, S. E.; Juhl, M. *Helv. Chim. Acta* **2002**, *85*, 3712−3736. (u) Denmark, S. E.; Gomez, L. *J. Org. Chem.* **2003**, *68*, 8015−8024. (v) van Berkom, L. W. A.; Kuster, G. J. T.; Kalmoua, F.; de Gelder, R.; Scheeren, H. W *Tetrahedron Lett.* **2003**, *44*, 5091−5093. (w) van Berkom, L. W. A.; Kuster, G. J. T.; Scheeren, H. W. *Mol. Diversity* **2003**, *6*, 271−282. (x) Denmark, S. E.; Montgomery, J. I. *Angew. Chem., Int. Ed.* **2005**, *44*, 3732−3736. (y) Denmark, S. E.; Montgomery, J. I.; Kramps, L. A. *J. Am. Chem. Soc.* **2006**, *128*, 11620−11630. (z) Denmark, S. E.; Baiazitov, R. Y. *J. Org. Chem.* **2006**, *71*, 593−605. (aa) Denmark, S. E.; Baiazitov, R. Y.; Nguyen, S. T. *Tetrahedron* **2009**, *65*, 6535−6548. (bb) van Berkom, L. W. A.; Kuster, G. J. T.; de Gelder, R.; Scheeren, H. W. *Eur. J. Org. Chem.* **2004**, 4397−4404. (cc) Kuster, G. J.; Scheeren, H. W. *Tetrahedron Lett.* **1998**, *39*, 3613−3616.

(4) Chataigner, I.; Piettre, S. R. *Org. Lett.* **2007**, *9*, 4159−4162.

(5) (a) Pugnaud, S.; Masure, D.; Hallé, J.-C.; Chaquin, P. *J. Org. Chem.* **1997**, *62*, 8687−8692. (b) Domingo, L. R.; Arnó, M.; Andrés, J. *J. Org. Chem.* **1999**, *64*, 5867−5875. (c) Celebi-Olcum, N.; Ess, D. H.; Aviyente, V.; Houk, K. N. *J. Org. Chem.* **2008**, *73*, 7472−7480.

(6) Denmark, S. E.; Seierstad, M.; Herbert, B. *J. Org. Chem.* **1999**, *64*, 884−901.

(7) (a) Domingo, L. R.; Asensio, A. *J. Org. Chem.* **2000**, *65*, 1076−1083. (b) Domingo, L. R. *Theor. Chem. Acc.* **2000**, *104*, 240−246.

(8) Avalos, M.; Babiano, R.; Bravo, J. L.; Cintas, P.; Jiménez, J. L.; Palacios, J. C.; Silva, M. A. *Chem.−Eur. J.* **2000**, *6*, 267−277.

(9) The differences leading to the regiochemical preference nevertheless remained weak, making the complete computational study of the competitive reaction paths important. The computation of the Fukui indices on the atomic AIM basins led to identical values for the two competing atoms in **1**, leading to the prediction of no regioselectivity.

		f^+	f^-
2	C(HH)	0.39	***0.46***
	C(HO)	0.41	***0.21***
1	O(N)	***0.20***	0.04
	C(HN)	***0.20***	0.11

(10) This highlights that reproduction of the exclusive obtention of nitrosoketal **E4** from an endo approach under high-pressure conditions from theoretical computations requires a special modeling approach, mostly centered on a proper modeling of the steric effects, that is not available currently for a routine quantum approach. See: Dumas, F.; Fressigne, C.; Langlet, J.; Giessner-Prettre, C. *J. Org. Chem.* **1999**, *64*, 4725−4732.

(11) Domingo, L. R.; Sáez, J. A. *Org. Biomol. Chem.* **2009**, *7*, 3576−3583.

(12) (a) Silvi, B.; Savin, A. *Nature* **1994**, *371*, 683−686. (b) Savin, A.; Silvi, B.; Colonna, F. *Can. J. Chem.* **1996**, *74*, 1088−1096.

(13) Berski, S.; Andrés, A.; Silvi, B.; Domingo, L. R. *J. Phys. Chem. A* **2006**, *110*, 13939−13947.

(14) Domingo, L. R.; Pérez, P.; Sáez, J. A. *Tetrahedron* **2013**, *69*, 107−114.

(15) This basin was designed by adding the valence basin between these two atoms and the monosynaptic basin at C3 to simplify the description. The monosynaptic basin on C3 cannot be associated with pseudoradical bond formation because it is located on a central atom of the heterodiene. A nongrouped description of the basins can be found in Figure FS1 in the Supporting Information.

(16) The interaction of **E1** and **E2** led to the formation of (**i**) unpublished results. For other homo domino processes, see: (a) Nesi,

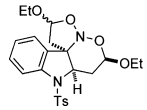

R.; Turchi, S.; Giomi, D.; Danesi, A. *Tetrahedron* **1999**, *55*, 13809−13818. (b) Giomi, D.; Turchi, S.; Danesi, A.; Faggi, C. *Tetrahedron* **2001**, *57*, 4237−4242. (c) Korotaev, V. Y.; Sosnovskikh, V. Y.; Barabanov, M. A.; Yasnova, E. S.; Ezhikova, M. A.; Kodess, M. I.; Slepukhin, P. A. *Tetrahedron* **2010**, *66*, 1404−1409.

(17) Denmark, S. E.; Cottell, J. In *Synthetic Applications of 1,3 Dipolar Cycloaddition Chemistry Toward Heterocycles and Natural Products*; Padwa, A., Pearson, W. H., Eds.; Wiley-Interscience: New York, 2002; pp 83−167.

(18) For the computed TS, the *s-cis* conformation for **3** (for the C=C−C=O system) led to lower energetic differences and was considered for this cycloaddition step.

(19) Bentabed-Ababsa, G.; Hamza-Reguig, S.; Derdour, A.; Domingo, L. R.; Sáez, J. A.; Roisnel, T.; Dorcet, V.; Nassare, E.; Mongin, F. *Org. Biomol. Chem.* **2012**, *10*, 8434−8444.

(20) (a) Polo, V.; Andres, J.; Castillo, R.; Berski, S.; Silvi, B. *Chem.—Eur. J.* **2004**, *10*, 5165−5172. (b) Domingo, L. R.; Sáez, J. A. *J. Org. Chem.* **2011**, *76*, 373−379.

(21) Gillet, N.; Chaudret, R.; Contreras-García, J.; Yang, W.; Silvi, B.; Piquemal, J.-P. *J. Chem. Theory Comput.* **2012**, *8*, 3993−3997.

(22) Frisch, M. J.; Trucks, G. W.; Schlegel, H. B.; Scuseria, G. E.; Robb, M. A.; Cheeseman, J. R.; Scalmani, G.; Barone, V.; Mennucci, B.; Petersson, G. A.; Nakatsuji, H.; Caricato, M.; Li, X.; Hratchian, H. P.; Izmaylov, A. F.; Bloino, J.; Zheng, G.; Sonnenberg, J. L.; Hada, M.; Ehara, M.; Toyota, K.; Fukuda, R.; Hasegawa, J.; Ishida, M.; Nakajima, T.; Honda, Y.; Kitao, O.; Nakai, H.; Vreven, T.; Montgomery, J. A., Jr.; Peralta, J. E.; Ogliaro, F.; Bearpark, M.; Heyd, J. J.; Brothers, E.; Kudin, K. N.; Staroverov, V. N.; Kobayashi, R.; Normand, J.; Raghavachari, K.; Rendell, A.; Burant, J. C.; Iyengar, S. S.; Tomasi, J.; Cossi, M.; Rega, N.; Millam, J. M.; Klene, M.; Knox, J. E.; Cross, J. B.; Bakken, V.; Adamo, C.; Jaramillo, J.; Gomperts, R.; Stratmann, R. E.; Yazyev, O.; Austin, A. J.; Cammi, R.; Pomelli, C.; Ochterski, J. W.; Martin, R. L.; Morokuma, K.; Zakrzewski, V. G.; Voth, G. A.; Salvador, P.; Dannenberg, J. J.; Dapprich, S.; Daniels, A. D.; Farkas, Ö.; Foresman, J. B.; Ortiz, J. V.; Cioslowski, J.; Fox, D. J. *Gaussian 09*, version B.01; Gaussian, Inc.: Wallingford, CT, 2009.

(23) (a) Lee, C.; Yang, W.; Parr, R. G. *Phys Rev. B* **1988**, *37*, 785−789. (b) Miehlich, B.; Savin, A.; Stoll, H.; Preuss, H. *Chem. Phys. Lett.* **1989**, *157*, 200−206. (c) Becke, A. D. *J. Chem. Phys.* **1993**, *98*, 5648−5652.

(24) Cossi, M.; Scalmani, G.; Rega, N.; Barone, V. *J. Chem. Phys.* **2002**, *117*, 43−54 and references therein.

(25) Lan, Y.; Zou, L.; Cao, Y.; Houk, K. N. *J. Phys. Chem. A* **2011**, *115*, 13906−13920 and references therein.

(26) Atkins, P. W. *Physical Chemistry*, 5th ed.; Oxford University Press: Oxford, 1994.

(27) (a) Boys, S. F.; Bernardi, F. *Mol. Phys.* **1970**, *19*, 553−566. (b) Simon, S.; Duran, M.; Dannenberg, J. J. *J. Chem. Phys.* **1996**, *105*, 11024−11031.

(28) (a) Becke, A. D.; Edgecombe, K. E. *J. Chem. Phys.* **1990**, *92*, 5397−5403. (b) Savin, A.; Nesper, R.; Wengert, S.; Fässler, T. F. *Angew. Chem., Int. Ed. Engl.* **1997**, *36*, 1808−1832.
(29) (a) Noury, S.; Krokidis, X.; Fuster, F.; Silvi, B. *Comput. Chem.* **1999**, *23*, 597−604. (b) Matito, E.; Silvi, B.; Duran, M.; Solà, M. *J. Chem. Phys.* **2006**, *125*, 024301. (c) Fexas, F.; Matito, E.; Duran, M.; Solà, M.; Silvi, B. *J. Chem. Theory Comput.* **2010**, *2010*, 2736−2742.